2nd URSI AT-RASC, Gran Canaria, 28 May – 1 June 2018

Bistatic ArcSAR

Massimiliano Pieraccini, and Lapo Miccinesi
Department of Information Engineering
University of Florence
Via Santa Marta, 3 50139 Firenze, Italy

Abstract

Since at least one decade GB-SAR (Ground Based Synthetic Aperture Radar) has been used for monitoring slopes and large structures. ArcSAR is a particular implementation of GBSAR, which has been receiving increasing interest in the last years. The great advantage of ArcSAR is its capability to synthesize images at 360° with constant resolution in azimuth. Nevertheless ArcSAR has a critical limitation: it detects only the displacement component along the range direction. In this paper the authors propose a radar technique that allows an ArcSAR to operate as bistatic radar. In this way the same radar equipment is able to acquire two images taken from different points of view, acquiring two different components of the displacement of the targets in the field of view.

1. Introduction

Ground Based Synthetic Aperture Radar (GB-SAR) is a well-known technique for monitoring landslides [1] and open pits [2], and for detecting small displacements of large structure like bridges [3] and dams [4]. The most common implementation of this kind of radar is based on a linear mechanical guide [1]. In 1989 Klausing [5] was the first to propose a radar (that he named ROSAR) able to exploit the rotatory movement to synthesize a large aperture. In recent years the interest in this kind of radar (currently named ArcSAR) is increased [6],[7],[8],[9],[10] because of its unique capability to synthesize images with constant resolution in azimuth.
ArcSAR systems are able to provide both images and displacement maps, but they detect only the component of displacement along the range direction. This can result a critical limitation in specific applications, as demonstrated by Severin et al. [3] in slope monitoring, and Dei et al. [4] in structural monitoring.
In this paper the authors propose to operate an ArcSAR as bistatic radar in order to detect two different components of the target displacement.
The basic principles of bistatic radar have long been known [11]. Furthermore, recently the same authors of this paper proposed a bistatic linear GBSAR [12] (i.e. based on a linear mechanical guide). Nevertheless no one before has proposed a bistatic ArcSAR.

2. The Working Principle of Bistatic ArcSAR

The working principle of bistatic ArcSAR is shown in Figure 1. A rotating radar head is provided with a second receiving channel that is linked to a transponder through a RF microwave cable.

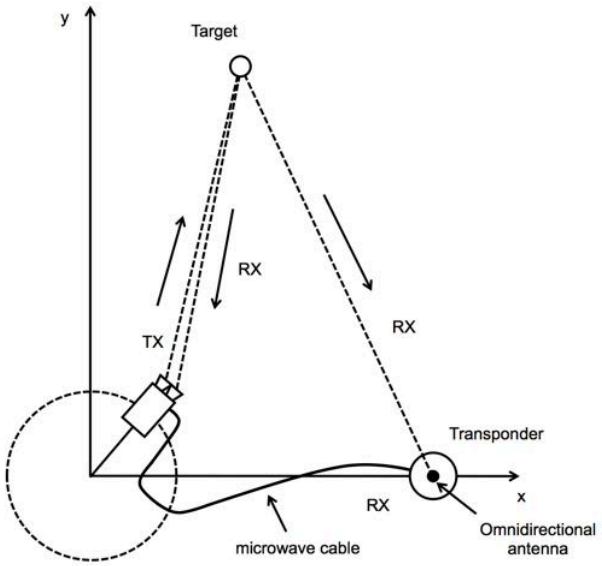

Figure 1. Working principle of Bistatic ArcSAR

The transponder consists of an amplifier stage and an omnidirectional antenna. By rotating the arm the radar acquires two images: 1) a monostatic image by transmitting and receiving with the two antennas of the radar head; 2) a bistatic image by transmitting with the antenna of the radar head and by receiving through the omnidirectional antenna of the transponder.
Bistatic SAR image can be focused through a back projection algorithm. With reference to Figure 1 the back projection is implemented compensating the phase history of any path radar-target-transponder-radar. On this basis we have modified the algorithm described in [9] (that was originally developed for monostatic ArcSAR) for operating in the bistatic modality as reported in [12].

3. Simulation

The echo of a point target in the position x_0 = 10 m, y_0 = 15 m was simulated. The transponder was positioned in x_T = 20 m, y_T = 0 m. The radius of ArcSAR was 1 m. The simulation parameter we used were: f_c = 10 GHz, B = 160 MHz, N_f=401, N_p=301. The rotating antenna was a horn and its angular pattern has been calculated using standard formulas [13]. The fixed antenna is assumed omnidirectional in the horizontal plane. Figure 2 shows the obtained focused image in log scale.

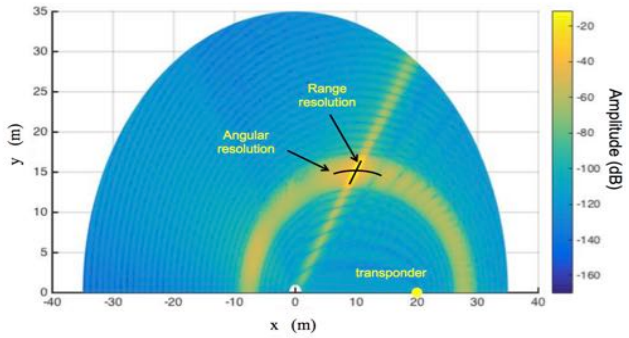

Figure 2. Simulated radar image of a point in (10 m , 15 m)

It is worth to note that range and angular resolutions are not in orthogonal directions, furthermore they are not constant in the image but they depend on the specific image point. Another unique feature of the bistatic configuration is that the point C (see also Figure 3) with respect to which the angular resolution is defined is not fixed, but is changing with the image point P. In effect it is the median point of the segment between the rotating antenna and the omnidirectional fixed antenna

4. Detecting 2D-Displacements

The specific advantage of a Bistatic ArcSAR is its capability to detect two components of the target displacement. As it is well known [1] interferometric radar is able to detect small displacements of a target (Δu) in its field of view by exploiting the relationship

$$\Delta u = \frac{\lambda}{4\pi}\Delta\phi \tag{1}$$

where $\Delta\varphi$ is the detected differential phase between two images taken before and after the displacement.
By acquiring monostatic and bistatic images of the same scenario (i.e. using the ArcSAR in monostatic and bistatic configuration) it is possible to obtain two components of the displacement: along the range direction Δu_1 (in monostatic configuration) and along the bisector direction Δu_2 (in bistatic configuration).

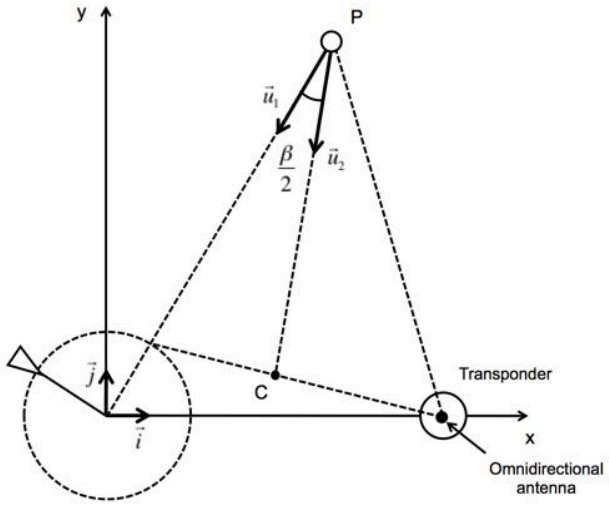

Figure 3. Detecting 2-D displacements

With reference to Figure 3 the detected displacements Δu_1 and Δu_2 are in linear relationship with the two orthogonal components Δx and Δy of the effective displacement:

$$\begin{pmatrix} \Delta u_1 \\ \Delta u_2 \end{pmatrix} = M \begin{pmatrix} \Delta x \\ \Delta y \end{pmatrix} \tag{2}$$

with

$$M = \begin{bmatrix} \cos\vartheta_x^{(1)} & \cos\vartheta_y^{(1)} \\ \cos\vartheta_x^{(2)} & \cos\vartheta_y^{(2)} \end{bmatrix} \tag{3}$$

$$\cos\vartheta_x^{(1)} = \frac{\vec{R}\cdot\vec{i}}{|\vec{R}|} \qquad \cos\vartheta_y^{(1)} = \frac{\vec{R}\cdot\vec{j}}{|\vec{R}|} \tag{4}$$

$$\cos\vartheta_x^{(2)} = \frac{(\vec{R}-\vec{R}_C)\cdot\vec{i}}{|\vec{R}-\vec{R}_C|} \qquad \cos\vartheta_x^{(2)} = \frac{(\vec{R}-\vec{R}_C)\cdot\vec{j}}{|\vec{R}-\vec{R}_C|} \tag{5}$$

Therefore

$$\begin{pmatrix} \Delta y \\ \Delta z \end{pmatrix} = M^{-1} \begin{pmatrix} \Delta u_1 \\ \Delta u_2 \end{pmatrix} \tag{6}$$

The later equation allows to calculate Δx and Δy from the measured displacements Δu_1 and Δu_2.

5. The Bistatic ArcSAR Prototype

Figure 4 shows a sketch of the radar prototype we assembled for testing the working principle of bistatic ArcSAR. A vector network analyzer (VNA) HP8720D operated as transceiver providing a continuous wave stepped frequency signal (SFCW) in X-band with central frequency f_c = 10 GHz and bandwidth B =160 MHz. Two RF cables linked the VNA to the front-end fixed at the tip of the rotating arm.

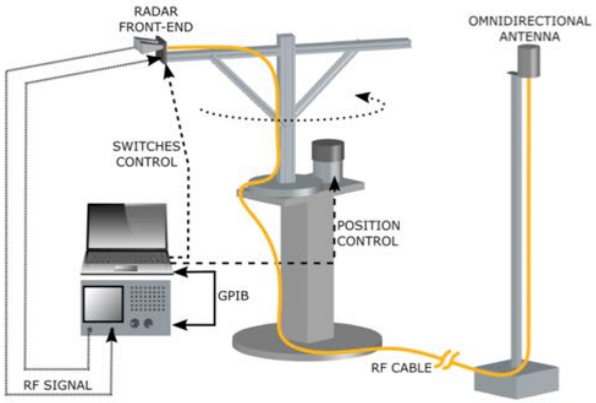

Figure 4. The radar prototype

With reference to the block scheme in Figure 5, two single-pole double-throw (SPDT) switches provided a direct path (through a -40 dB attenuator) that by-passed the antennas in order to perform calibrated measurements. The antennas were two horns which physical dimensions were 75 mm in width and 50 mm in height, 125 mm in length. Another SPDT before the receiving antenna switched the signal in a 25 m long RF cable. connected to a omnidirectional antenna. Two 40 dB amplifiers compensate the cable loss

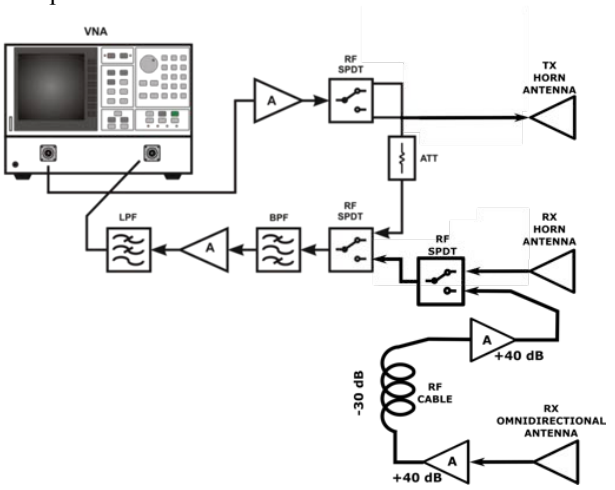

Figure 5. Block scheme

It is of note that while the monostatic measurements result calibrated through the direct path, the 15 m RF cable is out of the calibration loop. This could be a possible problem for the phase stability of the interferometric measurements. For mitigating it we used a high quality RF cable and we avoided any not necessary and not repeatable movement of the cable.

5. Experimental Test

For testing the capability to obtain monostatic and bistatic radar images we installed the ArcSAR and the transponder in a garden of the University (Figure 6).

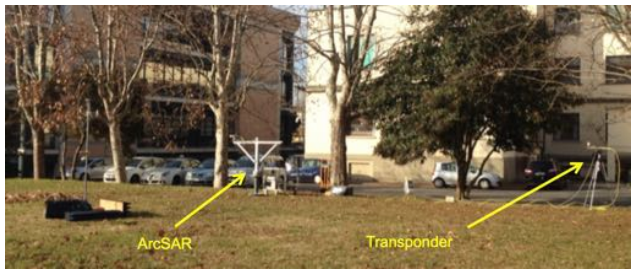

Figure 6. Picture of the radar installation

In front and on the side of the radar there was a metallic fence as reported in the map in Figure 7.

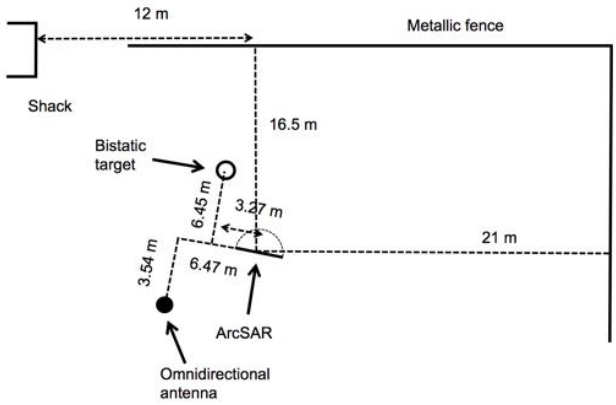

Figure 7. Map of the radar installation

Figure 8 and Figure 9 show the obtained monostatic and bistatic images.

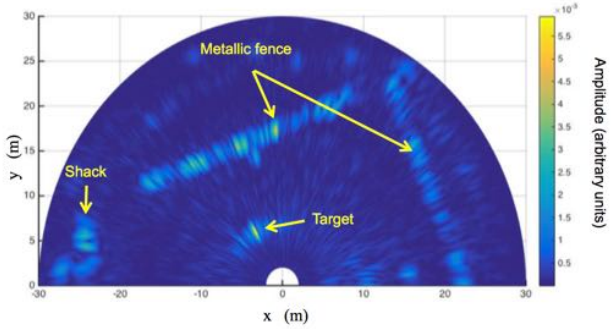

Figure 8. Monostatic image

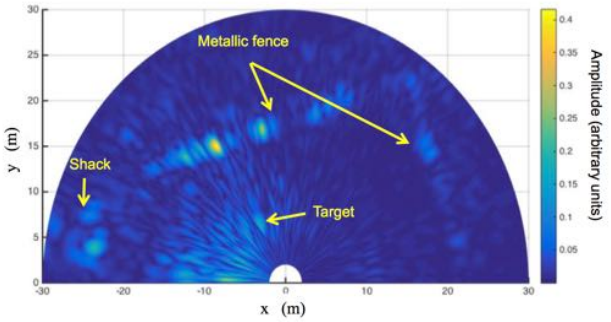

Figure 9. Bistatic image

Both images appear of good quality. As expected the resolution and the signal-to-noise ratio of the monostatic image are better.
With the aim to proof the capability of the bistatic radar to detect two components of the displacement a special target was assembled (Figure 10).

Figure 10. Picture of the bistatic target

At a metallic pole we fixed some metallic arms for simulating an occasional target and to increase its radar cross section. The pole was mounted over a linear micrometric positioner for optical bench with 0.1 mm nominal accuracy. Some eccosorb panels were used to cover both the mechanical device and a dead load that kept stable the base of the target. The positioner was aligned along the *y*-axis. A reference couple of images (monostatic and bistatic) was acquired. Aftermath, the positioner was moved of 10 mm along *y*-axis, and a second couple of images was acquired. The obtained displacements along *y* and *x* were +1.1 mm and -7.61 mm (the nominal values were 0.0 mm and -10 mm). The agreement is not perfect but the working principle has been demonstrated.

5. Conclusion

The working principle of a bistatic ArcSAR based on a transponder linked to the main radar through a microwave cable, has been demonstrated. Nevertheless the use of RF cable could give problems in the in-field application of this system, as it could give uncontrolled phase shift if inadvertently moved. Furthermore, the attenuation of a RF cable is very high. An alternative solution more suitable for the in-field application could be based on a RF link realized with two antennas, one of which has to be provided with a rotary joint to keep the alignment when the ArcSAR rotates around its axes.

7. References

1. M. Pieraccini, L. Noferini, D. Mecatti, C. Atzeni, G. Teza, A. Galgaro, Z. Zaltron, "Integration of radar interferometry and laser scanning for remote monitoring of an urban site built on a sliding slope," *IEEE Transactions on geoscience and remote sensing*, **44**, 9, September 2009, pp. 2335-2342.
2. G. Luzi, M. Pieraccini, D. Mecatti, L. Noferini, G. Macaluso, A. Tamburini, C. Atzeni, "Monitoring of an alpine glacier by means of ground-based SAR interferometry", *IEEE Geoscience and Remote Sensing Letters*, **4**, 3, July 2007, pp. 495-499,
3. J. Severin, E. Eberhardt, L. Leoni, S. Fortin, "Development and application of a pseudo-3D pit slope displacement map derived from ground-based radar." *Engineering Geology*, **181**, 2014, pp. 202-211
4. D. Dei, D. Mecatti, M. Pieraccini, "Static Testing of a Bridge Using an Interferometric Radar: The Case Study of "Ponte degli Alpini," Belluno, Italy," *The Scientific World Journal*, 2013.
5. W. Jenkins, B. Rosenblad, F. Gomez, J. Legarsky, and E. Loehr, "Deformation measurements of earth dams using a ground based interferometric radar," 2012 ASDSO Annual Conference on Dam Safety, p. 15, Denver, Colo, United States, September 2012.
6. H. Klausing, "Feasibility of a Synthetic Aperture Radar with Rotating Antennas (ROSAR)", 9th European Microwave Conference, 4-7 Sept. 1989, pp. 287 – 299
7. Y. Luo, H. Song, R. Wang, Y. Deng, F. Zhao, Z. Xu, "Arc FMCW SAR and Applications in Ground Monitoring" *IEEE Transactions on Geoscience and Remote Sensing*, **52**, 9, 2014, pp. 5989-5998,
8. H. Lee, J. H., Lee, K. E. Kim, N. H. Sung, S. J. Cho, "Development of a truck-mounted arc-scanning synthetic aperture radar," *IEEE Transactions on Geoscience and Remote Sensing*, **52**, 5, 2014, p. 2773-2779.
9. M. Pieraccini, L. Miccinesi, ArcSAR: Theory, Simulations, and Experimental Verification, *IEEE Transactions on Microwave Theory and Techniques*, **65**, 1, January 2017, pp. 293 – 301,
10. Huang, Z., Sun, J., Tan, W., Huang, P., & Han, K. "Investigation of Wavenumber Domain Imaging Algorithm for Ground-Based Arc Array SAR," *Sensors*, **17**, 12, 2017, p. 2950.
11. N. J. Willis, "Bistatic Radar" SciTech Publishing
12. M. Pieraccini, L. Miccinesi, N. Rojhani, "A GBSAR Operating in Monostatic and Bistatic Modalities for Retrieving the Displacement Vector." *IEEE Geoscience and Remote Sensing Letters*, **14**, 9, Sept. 2017, pp. 1494 – 1498
13. C. A. Balanis, Antenna Theory: Analysis and Design, 3rd ed. Hoboken, NJ, USA: Wiley,